Int. J. Heat Mass Transfer. Vol. 24, pp. 231–241
Pergamon Press Ltd. 1981. Printed in Great Britain

0017-9310/81/0201-0231 $02.00/0

A MATHEMATICAL MODEL OF NOZZLE BLOCKAGE BY FREEZING

P. SAMPSON and R. D. GIBSON

Department of Mathematics, Statistics and Computing,
Newcastle upon Tyne Polytechnic, Newcastle upon Tyne NE1 8ST, U.K.

(*Received* 5 *November* 1979 *and in revised form* 15 *June* 1980)

Abstract—A mathematical model is presented which describes the formation of a crust on the inside of a cold pipe through which a fluid is flowing. A numerical/analytical treatment of the inward solidification problem is given and criteria presented which predict conditions under which blockage will occur.

NOMENCLATURE

B,	freezing parameter;
C,	specific heat of fluid/solid;
$C_nR_n'(1)$,	nth coefficient in series (52);
$D(t)$,	defined (31);
$d(t)$,	perturbation of $D(t)$ (58);
$f(z,t)$,	heat flux series (52);
f,	friction factor;
$g(z)$,	spatial part of perturbation γ (61);
H,	latent heat of fusion;
k_f,	thermal conductivity of liquid;
k_s,	thermal conductivity of solid;
l_0,	length of pipe;
P,	pressure drop over pipe;
p,	fluid pressure;
Pe,	Peclet number;
Pe_0,	Peclet number at $t = 0$;
$Q(t)$,	volume flux in (1);
R,	crust dependent radial coordinate (42);
Re,	Reynolds number;
r,	radial coordinate;
T,	temperature;
t,	time;
u,	radial velocity;
w,	axial velocity;
z,	axial coordinate;
α,	pressure parameter (33) or (38);
Γ,	square of δ;
γ,	perturbation of Γ;
δ,	radial position of crust;
θ,	temperature;
κ,	thermal diffusivity of fluid $(=k_f/\rho C)$;
λ_n,	nth eigenvalue in series (52);
ν,	kinematic viscosity of fluid;
ρ,	density of fluid/solid;
σ,	perturbation growth rate (61).

Subscripts

m,	at fluid/solid interface;
0,	at pipe entrance;
s,	at steady state;
w,	at pipe wall.

Superscripts

(1),	stable solution;
(2),	unstable solution;
*,	dimensional variable.

INTRODUCTION

RECENTLY, the problem of the solidification of a warm liquid as it flows through a pipe, the walls of which are maintained at a uniform sub-freezing temperature, has received considerable attention. This type of solidification process arises in the flow of liquid metals through a nozzle and the ensuing formation of a solid crust on the nozzle walls. If conditions are sufficiently severe, the nozzle may block.

The seminal paper in this field is due to Zerkle and Sunderland [1]. It is concerned with laminar flow with a prescribed constant inlet velocity and the pressure drop down the pipe which is required to maintain the inlet velocity as the crust is formed is calculated from this. However, the analysis does not cover the important case of blockage. A later paper by Des Ruisseaux and Zerkle [6] did consider blockage criteria. Epstein, Yim and Cheung [2] considered the flow rate and penetration of the fluid by prescribing a power-law description of the solidified crust. The results of their numerical analysis were compared with experimental measurements.

Özisik and Mulligan [3] investigated both transient and steady state models with a slug-flow velocity profile in the axial direction and no radial convection. Martinez and Beaubouef [4] presented a laminar flow model with radial and axial velocities prescribed from the continuity and momentum equations.

In the current investigation, a laminar velocity prescription will be used, as in [4]. The maintained pressure gradient along the pipe is assumed constant, so that as the crust thickness and viscous resistance increases, the inlet speed decreases. In fact, it is shown that the governing equations are non-linear and integro-differential in character; it will also be shown that under certain conditions, the steady-state equations have no solution. Finally, from the analysis of the time-dependent model, a simple criterion will be presented to predict whether a given system will lead to

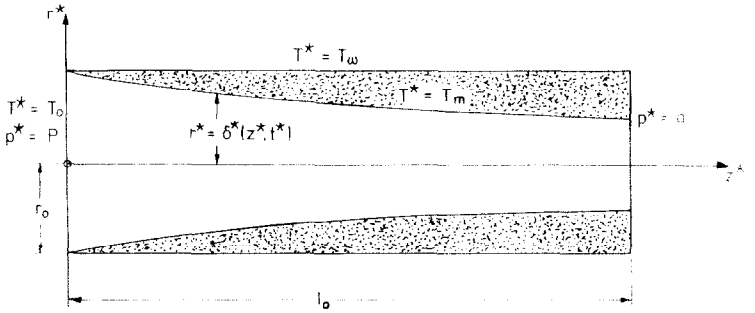

FIG. 1.

nozzle blockage, and a brief comparison with some experimental results with water due to Des Ruisseaux and Zerkle is made, showing good agreement.

THE HYDRODYNAMIC MODEL

A cylindrical pipe of length l_0 and radius r_0 has its wall maintained at a constant temperature (T_w) below the freezing temperature (T_m) of a fluid which is forced through the pipe by a maintained pressure drop (P) over the ends of the pipe. The fluid loses heat to the colder wall and starts to solidify, forming a crust on the tube wall. The fluid temperature at the inlet is assumed constant and uniform at a value T_0, greater than the melting temperature. Without loss of generality, the outlet pressure may be assumed zero.

The densities of the fluid and solid phases are assumed to be identical and constant, denoted by ρ. The thermal conductivities of fluid and solid (k_f and k_s, respectively) the kinematic viscosity (ν), the specific heat (C) of the fluid and the latent heat of fusion (H), are all assumed constant.

We are concerned with the growth of the solidified crust and so propose that the equations of momentum, continuity and thermal energy are those of steady-state, since the fluid motion will adapt itself to the changing crust much more quickly than the crust can change. Nevertheless, the fluid temperature and motion are time-dependent, via the crust, but quasi-steadily so. This is the standard approximation for large Stefan numbers, corresponding to the fact that the timescale associated with the motion of the interface is longer than either the thermal or viscous timescales. We have axial and radial velocity fields, respectively w^*, and u^*, defined as

$$w^*(r^*, z^*, t^*) = 2Q(t^*)\delta^{*-2}(z^*, t^*) \times (1 - r^{*2}\delta^{*-2}(z^*, t^*)) \quad (1)$$

$$u^*(r^*, z^*, t^*) = (r^*/\delta^*)(\partial\delta^*/\partial z^*)w^* \quad (2)$$

where $r^* = \delta^*(z^*, t^*)$ gives the position of the solid/liquid interface and $Q(t^*)$ is determined below. These fields satisfy the mass continuity equation and the no-slip condition at $r^* = \delta^*$, (see [4]). We define a local Reynolds number

$$Re = 2Q(t^*)/\nu\delta^* \quad (= 2\delta^*\bar{w}^*/\nu) \quad (3)$$

based on local pipe diameter and local bulk axial velocity $\bar{w}^*$. We similarly define a local Peclet number

$$Pe = 2Q(t^*)/\kappa\delta^* \quad (= 2\delta^*\bar{w}^*/\kappa). \quad (4)$$

The local bulk axial velocity (radially averaged) is

$$\bar{w}^*(z^*, t^*) = \delta^{*-2}\int_0^{\delta^*} 2r^*w^*(r^*, z^*, t^*)\mathrm{d}r^*; \quad (5)$$

that is

$$\bar{w}^*(z^*, t^*) = Q(t^*)/\delta^{*2}(z^*, t^*). \quad (6)$$

The equation for the pressure drop down the pipe is the familiar

$$\frac{\partial p^*}{\partial z^*} = \frac{-\rho f \bar{w}^{*2}}{4\delta^*} \quad (7)$$

where in the case of laminar flow the friction factor, f, is given by

$$f = 64/Re \quad (8)$$

and so

$$\frac{\partial p^*}{\partial z^*} = \frac{-8\rho\nu Q(t^*)}{\delta^{*4}(z^*, t^*)}. \quad (9)$$

Equation (9) has to satisfy the following boundary conditions

$$p^*(0, t^*) = P \quad (10)$$

$$p^*(l_0, t^*) = 0 \quad (11)$$

and in order to satisfy these conditions, $Q(t^*)$ must be given by

$$Q(t^*) = \frac{P}{8\rho\nu\int_0^{l_0}\delta^{*-4}(x^*, t^*)\mathrm{d}x^*} \quad (12)$$

giving the fluid pressure

$$p^*(z^*, t^*) = P\frac{\int_{z^*}^{l_0}\delta^{*-4}(x^*, t^*)\mathrm{d}x^*}{\int_0^{l_0}\delta^{*-4}(x^*, t^*)\mathrm{d}x^*}. \quad (13)$$

It is clear from (12) and (13) that both the fluid pressure and velocity depend upon the crust over the

entire length of the pipe. It should also be noted that if δ^* is a monotonically decreasing function of t^* then $Q(t^*)$ will be a monotonically decreasing function of t^*, and so the inlet velocity will decrease as the crust thickens.

THE THERMODYNAMIC MODEL

The quasi-steady heat-transfer model for the fluid is

$$u^*\frac{\partial T^*}{\partial r^*} + w^*\frac{\partial T^*}{\partial z^*} = \kappa\left(\frac{\partial^2 T^*}{\partial r^{*2}} + \frac{1}{r^*}\frac{\partial T^*}{\partial r^*} + \frac{\partial^2 T^*}{\partial z^{*2}}\right) \tag{14}$$

for $0 < r^* < \delta^*$ and $0 < z^* < l_0$. For the solid region, we have

$$\frac{\partial^2 T^*}{\partial r^{*2}} + \frac{1}{r^*}\frac{\partial T^*}{\partial r^*} + \frac{\partial^2 T^*}{\partial z^{*2}} = 0 \tag{15}$$

for $\delta^* < r^* < r_0$ and $0 < z^* < l_0$. Equations (14) and (15) are to be solved subject to the conditions

$$T^*(r^*, 0, t^*) = T_0 \tag{16}$$

$$T^*(\delta^*, z^*, t^*) = T_m \tag{17}$$

$$T^*(r_0, z^*, t^*) = T_w \tag{18}$$

$$\rho H\frac{\partial \delta^*}{\partial t^*} = k_s\frac{\partial T^*}{\partial r^*}\bigg|_{r^*=\delta^{*+}} - k_f\frac{\partial T^*}{\partial r^*}\bigg|_{r^*=\delta^{*-}} \tag{19}$$

At this point, it is convenient to non-dimensionalise the equations. We use the following scalings

$$\delta^*(z^*, t^*) = r_0\delta(z, t) \tag{20}$$

$$T^*(r^*, z^*, t^*) = T_m + (T_0 - T_m)\theta(r, z, t) \tag{21}$$

where the independent variables are scaled

$$r^* = r_0 r \tag{22}$$

$$z^* = 2Q(0)z/\kappa \tag{23}$$

$$t^* = \rho H r_0^2 t/2k_f(T_0 - T_m) \tag{24}$$

to obtain

$$\frac{1}{\delta^2}\left(1 - \frac{r^2}{\delta^2}\right)\left(\frac{r}{\delta}\frac{\partial\delta}{\partial z}\frac{\partial\theta}{\partial r} + \frac{\partial\theta}{\partial z}\right) = D(t)\left(\frac{\partial^2\theta}{\partial r^2} + \frac{1}{r}\frac{\partial\theta}{\partial r} + \frac{1}{Pe_0^2}\frac{\partial^2\theta}{\partial z^2}\right) \tag{25}$$

for $0 < r < \delta$ and $0 < z < \alpha$, with

$$\frac{\partial^2\theta}{\partial r^2} + \frac{1}{r}\frac{\partial\theta}{\partial r} + \frac{1}{Pe_0^2}\frac{\partial^2\theta}{\partial z^2} = 0 \tag{26}$$

for $\delta < r < 1$ and $0 < z < \alpha$ subject to

$$\theta(r, 0, t) = 1 \tag{27}$$

$$\theta(\delta, z, t) = 0 \tag{28}$$

$$\theta(1, z, t) = -\theta_w \tag{29}$$

and the interface condition

$$2\frac{\partial\delta}{\partial t} = \frac{k_s}{k_f}\frac{\partial\theta}{\partial r}\bigg|_{r=\delta^+} - \frac{\partial\theta}{\partial r}\bigg|_{r=\delta} \tag{30}$$

where

$$D(t) = Q(0)/Q(t) = \frac{1}{\alpha}\int_0^\alpha \frac{dz}{\delta^4(z,t)} \tag{31}$$

$$Pe_0 = 2Q(0)/\kappa r_0 = Pe \quad \text{at } t = 0 \tag{32}$$

$$\alpha = \kappa l_0/2Q(0) = l_0/r_0 Pe_0 \tag{33}$$

$$\theta_w = (T_m - T_w)/(T_0 - T_m). \tag{34}$$

We have the boundary and initial conditions on δ

$$\delta(0, t) = 1 \tag{35}$$

$$\delta(z, 0) = 1 \tag{36}$$

so that from (12);

$$Q(0) = Pr_0^4/8\rho\nu l_0 \tag{37}$$

$$\alpha = 4\rho\nu\kappa l_0^2/Pr_0^4 \tag{38}$$

$$Pe_0 = Pr_0^3/4\rho\nu\kappa l_0. \tag{39}$$

In this analysis, the Peclet number is assumed to be large enough to justify the neglect of axial conduction in (25) and (26). This is consistent with the small slope of the solid/liquid interface, that is $\partial\delta^*/\partial z^*$ is of order $(1/Pe_0)$. In the important case of blockage, the large Peclet number expansion will break down when δ is of order $1/Pe_0$. A different scaling is required here, together with consideration of an asymptotic match between the outer solution outlined above and an inner expansion. This inner expansion would have to include axial conduction and time rates of change of temperature since progress towards blockage becomes very rapid. The analysis involved in this procedure is complicated (see, for example, Stewartson *et al.* [7]). Nevertheless, the present analysis provides the leading term in the asymptotic expansion and the results given are to be interpreted in this sense.

A case of practical interest is the flow of liquid steel through a tundish nozzle. Since for liquid metals the Prandtl number (ν/κ) is small, then it follows that the Reynolds number $(Re = \kappa Pe/\nu)$ is large. This then implies that the flow is turbulent and the present analysis must be considered as only a first approximation. (The authors intend to return to the case of turbulent flow in a later publication.)

By neglecting terms of order $(1/Pe_0^2)$, equation (26) with (28) and (29) has the solution

$$\theta(r, z, t) = \theta_\omega\frac{\ln(r/\delta(z,t))}{\ln\delta(z,t)}. \tag{40}$$

It then remains to solve (25) subject to (27), (28) and (30). This system is complicated by the presence of δ in (25) and (30), coupling these two equations in a complex way. To simplify matters, we remove the moving boundary by writing

$$\theta(r, z, t) \to T(R, z) \tag{41}$$

via

$$r = R\delta(z, t) \tag{42}$$

which has the following effect on derivatives

$$\frac{\partial}{\partial r} \rightarrow \frac{1}{\delta}\frac{\partial}{\partial R} \tag{43}$$

$$\frac{\partial}{\partial z} \rightarrow \frac{\partial}{\partial z} - \frac{R}{\delta}\frac{\partial \delta}{\partial z}\frac{\partial}{\partial R} \tag{44}$$

and so equations (25), (27), (28) and (30) become respectively

$$(1 - R^2)\frac{\partial T}{\partial z} = D(t)\left\{\frac{\partial^2 T}{\partial R^2} + \frac{1}{R}\frac{\partial T}{\partial R}\right\} \tag{45}$$

$$T(R,0) = 1 \tag{46}$$

$$T(1,z) = 0 \tag{47}$$

$$2\frac{\partial \delta}{\partial t} = \frac{B}{\delta \ln \delta} - \frac{1}{\delta}\frac{\partial T}{\partial R}\bigg|_{R=1} \tag{48}$$

where we have ignored axial conduction in (25), used (40) in (30) to obtain (48) and where

$$B = \frac{k_s}{k_f}\theta_w. \tag{49}$$

Equation (45) with boundary conditions (46) and (47) is the Graetz–Nusselt problem for an isothermal wall which was investigated by Sellars *et al.* [5]. The equation is modified by the presence of $D(t)$, admittedly dependent on δ, which affects their analysis only parametrically. For a given $D(t)$, (45) can be solved and an expression for $\partial T/\partial R$ at $R = 1$ evaluated and used in (48) to find δ at the next time step. A new value for $D(t)$ can then be calculated. The initial conditions are given by equation (36) and by implication and definition (31), $D(0) = 1$. There are two independent dimensionless parameters which determine the position of the crust, namely α and B.

THE CRUST

This analysis is concerned primarily with the development of the solid crust and so all that is needed is an expression for $\partial T/\partial R$ at $R = 1$. This can be obtained either by direct numerical integration of (45), which can be considered independent of time, or by further analysis. Alternatively, one can take advantage of the work done by Sellars *et al.* [5] on the classical Graetz problem and use

$$\left(\frac{\partial T}{\partial R}\right)_{R=1} = \sum_{n=0}^{\infty} C_n R_n'(1)\mathrm{e}^{-\lambda_n^2 D(t)z} = f(z,t) \tag{50}$$

where the C_n, $R_n'(1)$ and λ_n are provided by the aforementioned party for $n = 0$ to 9 and one may use the asymptotic solutions [5] for $n > 9$.

This series is derived from the solution to (45)–(47) which is

$$T(r,z) = \sum_{n=0}^{\infty} C_n R_n(r)\mathrm{e}^{-\lambda_n^2 Dz} \tag{51}$$

where R_n satisfies the homogeneous differential equation

$$rR_n'' + R_n' + \lambda_n^2 r(1 - r^2)R_n = 0 \tag{52}$$

with $R_n(1) = 0$, $R_n(0) = 1$ and $R_n'(0) = 0$.

For small $zD(t)$, the series in (50) is slowly convergent and since we expect α to be small in certain cases of experimental interest, it will be more useful to have an expression for $(\partial T/\partial R)_{R=1}$ as $z \rightarrow 0$. This was determined to be

$$\left(\frac{\partial T}{\partial R}\right)_{R=1} \rightarrow 0.670792 - 0.678325(Dz)^{-1/3} \text{ as } Dz \rightarrow 0 \tag{53}$$

from a least-squares fit to (50) for small z.

Having calculated $(\partial T/\partial R)_{R=1}$, analysis shows that a phase-plane plot of $\partial\delta/\partial t$ vs δ at a given distance down the pipe has two distinct sets of curves (see Fig. 2). The top curve (i) clearly shows two possibilities for steady-state solution where it crosses the δ axis. The path is from right to left as time increases and δ will reach δ_s after a time t_s. This is apparently a stable steady-state solution. There is no way to reach the point (*). Curve (ii) shows a trajectory for which there is no steady-state solution and in this case the pipe will block. The critical case where the δ axis is tangent to the curve is technically unstable since $\partial\delta/\partial t$ is always less than or equal to zero but numerical evidence indicates that an infinite time would be needed to reach the tangent.

In principle, for a given B and α, a curve for $\delta(\alpha, t)$ could be quickly produced without having to solve the differential equation (48) for δ. However, since the right hand size of (48) depends upon z and $D(t)$, which in turn depends on the crust over the entire length of the pipe, a numerical solution of (48) is necessary. Additionally, if one required to know the time taken to reach a steady-state, a phase-plane plot alone would not give this. Since equation (48) is integro-differential, we examine the critical points in the phase-plane in greater depth.

STABILITY OF SOLUTIONS

Equation (48) was first solved in conjunction with (45) for the steady state crust. It was solved with fifteen radial grid points by the method of lines using a

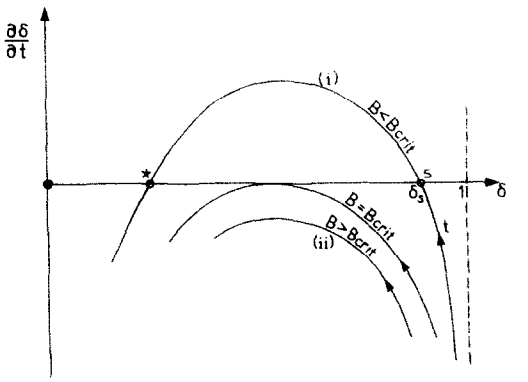

FIG. 2.

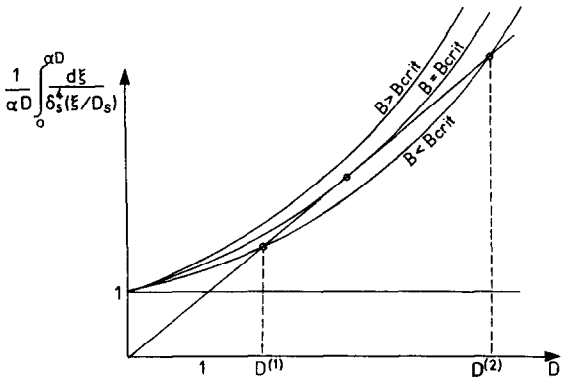

FIG. 3.

standard IBM Application Package, the System/360 Continuous System Modelling Program (CSMP). The independent variable z was rescaled as Dz to avoid repetition of the calculations. The only parameter to vary was B. The rescaling of z meant that for a given α and B, the equation

$$D = \frac{1}{\alpha D}\int_0^{zD} \frac{d\xi}{\delta_s^4(\xi/D)}$$

has to be solved for D. The right hand side of this equation is a monotonically increasing function of αD starting at the value 1 when $\alpha D = 0$. It can be seen from Fig. 3 that, as predicted, there are either two, one or no solutions to this equation depending on the value of B. The double solution was noted, in terms of two distinct Reynolds Numbers, by Des Ruisseaux and Zerkle [6] and they stated that only one solution was stable.

For a given α with $B < B_{crit}$, two values of D return two possible steady state configurations for the crust. The larger value of D would result from a crust which had encroached further into the liquid. It is maintained that the crust would never actually reach this state and would stop development at the lower value of D. This may seem clear from Fig. 2; however, Fig. 2 shows only the phase plane of the value of the crust at the end of the pipe. In fact, we need to show that the point marked S is stable in the entire 'phase-continuum' for all z since (48) is an integro-differential equation. This is a fairly straightforward but lengthy process.

Equation (48) can be written as

$$\frac{\partial \Gamma}{\partial t} = \frac{2B}{\ln \Gamma} + f(z,t) \quad \text{for } 0 \le z \le \alpha \text{ and } 0 \le t \tag{54}$$

where

$$\Gamma = \delta^2 \quad \text{and} \quad D(t) = \frac{1}{\alpha}\int_0^{\alpha} \frac{dz}{\Gamma^2(z,t)}. \tag{55}$$

It is known that as $z \to 0$

$$f = 0(z^{-1/3}) \quad \text{and} \quad \Gamma(z,t) \to 1$$

and as $z \to \infty$

$$f = 0(e^{-kz})$$

and that f is monotonically decreasing with z. If we assume a steady state solution given by $\Gamma = \Gamma_s(z)$ and $D = D_s$ then

$$\frac{2B}{\ln \Gamma_s} + f_s(z) = 0 \tag{56}$$

i.e. $\Gamma_s = \exp[-2B/f_s(z)]$

and so

$$D_s = \frac{1}{\alpha}\int_0^{\alpha} \exp[4B/f_s(z)]\,dz$$

or

$$D_s = \frac{1}{\alpha D_s}\int_0^{D_s} \exp[4B/f_s(z/D_s)]\,dz. \tag{57}$$

Equation (57) has two, one or no solutions for D_s, as depicted in Fig. 3, since f_s is monotonically decreasing, and so the right hand side is monotonically increasing from the value one. We now perturb this solution and set

$$D(t) = D_s + d(t);\ \Gamma(z,t) = \Gamma_s(z) + \gamma(z,t) \tag{58}$$

and this gives, from (54)–(56) as γ and d are small

$$\frac{\partial \gamma}{\partial t} = \frac{-2B\gamma}{\Gamma_s \ln^2 \Gamma_s} + \frac{z d(t)}{D_s}\frac{df_s}{dz} \tag{59}$$

$$d = \frac{-2}{\alpha}\int_0^{\alpha} \frac{\gamma(z,t)\,dz}{\Gamma_s^3(z)}. \tag{60}$$

Introducing normal modes by letting

$$\gamma(z,t) = e^{\sigma t} g(z)$$

where σ is the growth rate, then

$$\left(\sigma + \frac{2B}{\Gamma_s \ln^2 \Gamma_s}\right) g(z) = -\frac{2z}{\alpha D_s}\frac{df_s}{dz}\int_0^{\alpha} \frac{g(z)\,dz}{\Gamma_s^3(z)}. \tag{61}$$

This is a homogeneous integral equation for the eigenvalue σ with separable kernel and can be solved in a standard manner.

The integral on the right hand side of (61) is a constant, albeit unknown, which we denote by G and so (61) yields

$$\frac{g(z)}{\Gamma_s^3(z)} = -\frac{2Gz(df_s/dz)}{\alpha D_s \Gamma_s^3(\sigma + 2B/\Gamma_s \ln^2 \Gamma_s)}. \tag{62}$$

We then integrate (62) from $z = 0$ to $z = \alpha$ and the condition for a non-trivial solution is

$$1 = \frac{-2}{\alpha}\int_0^{\alpha} \frac{(z/D_s)(df_s/dz)\,dz}{\Gamma_s^3(\sigma + 2B/\Gamma_s \ln^2 \Gamma_s)} \tag{63}$$

which determines σ.

Substituting for $\Gamma_s(z)$ from (56) in the integral then gives

$$1 = \frac{-4B}{\alpha D_s} \int_0^z \frac{z(df_s/dz)\exp(6B/f_s(z))dz}{2B\sigma + f_s^2(z)\exp(2B/f_s(z))}. \quad (64)$$

If $\sigma \equiv 0$ we recover

$$1 = \frac{-4B}{\alpha D_s} \int_0^z x \exp[4B/f_s(x)] \frac{df_s}{dx} \frac{dx}{f_s^2(x)} \quad (65)$$

which can be integrated by parts, in conjunction with (57), to give

$$D_s = \frac{1}{2}\exp[4B/f_s(\alpha)] \quad \text{when } \sigma = 0. \quad (66)$$

Note that this equation can be obtained directly from (57) by differentiation with respect to D_s and so (66) corresponds to the critical case of the single (repeated) root solution to (57).

When (57) has two distinct roots, $D_s^{(1)}$ and $D_s^{(2)}$ ($> D_s^{(1)}$), it is fairly clear that for the same α and B there exists a unique solution D_s^+ to (66) for which $D_s^{(1)} < D_s^+ < D_s^{(2)}$, although D_s^+ does not of course satisfy (57). It is also apparent that

$$D_s^{(1)} > \frac{1}{2}\exp(4B/f_s^{(1)}(\alpha)) \quad (67)$$

and

$$D_s^{(2)} < \frac{1}{2}\exp(4B/f_s^{(2)}(\alpha)). \quad (68)$$

We now assume that σ is positive, then equation (64) gives

$$1 = \frac{-4B}{\alpha D_s^{(1)}} \int_0^z \frac{z(df_s^{(1)}/dz)\exp(6B/f_s^{(1)})dz}{2B\sigma + f_s^{(1)2}\exp(2B/f_s^{(1)})}$$

$$< \frac{-4B}{\alpha D_s^{(1)}} \int_0^z \frac{z(df_s^{(1)}/dz)\exp(4B/f_s^{(1)})dz}{f_s^{(1)2}}$$

$$= \frac{1}{D_s^{(1)}}\exp(4B/f_s^{(1)}(\alpha)) - 1$$

i.e. $D_s^{(1)} < \frac{1}{2}\exp(4B/f_s^{(1)}(\alpha))$.

This contradicts (67) and so $D_s^{(1)}$ cannot satisfy (64) for positive σ, hence $D_s^{(1)}$ represents a stable crust. The above and following arguments depend upon the quantity $\sigma + 2B/\Gamma_s \ln^2 \Gamma_s$ being positive, otherwise the inequalities would be reversed. If this were not so, equation (63) would admit no real solutions for D_s since $df_s/dz < 0$ for $z > 0$. Equation (63) could conceivably have real solutions for D_s if the quantity $\sigma + 2B/\Gamma_s \ln^2 \Gamma_s$ changed sign but then $g(z)$ would be unbounded when this happened, as indicated by (68).

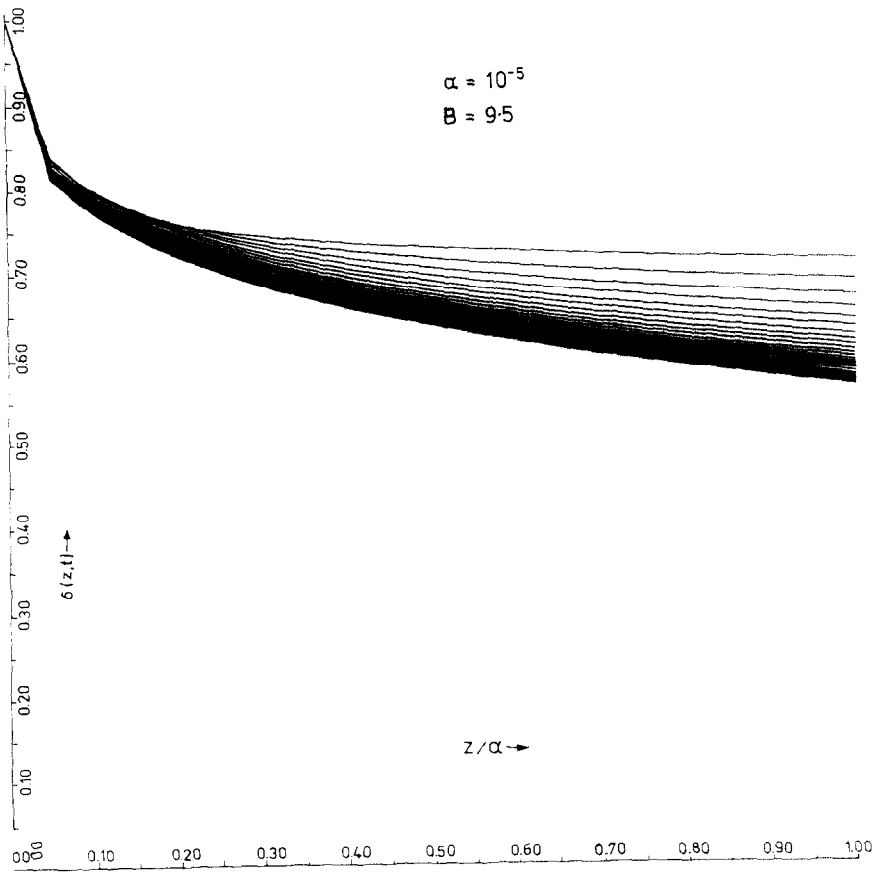

FIG. 4.

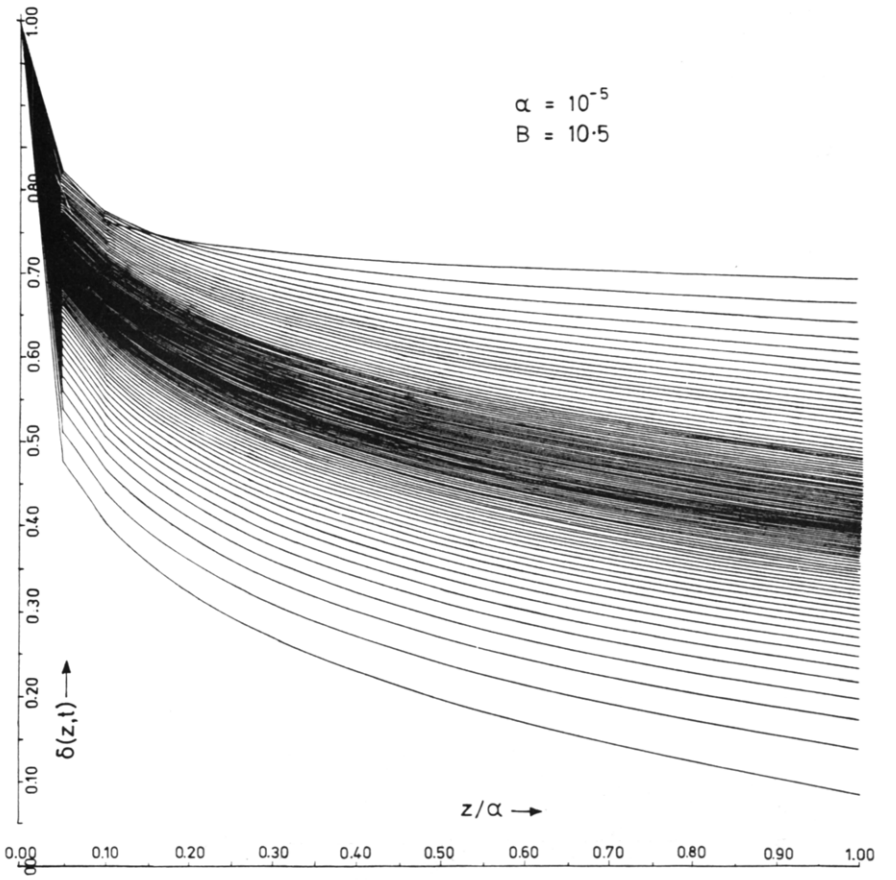

FIG. 5.

Next, assume that $D_s^{(2)}$ is a stable solution with $\sigma < 0$; then (64) gives

$$1 = \frac{-4B}{\alpha D_s^{(2)}} \int_0^{\alpha} \frac{z(\mathrm{d}f_s^{(2)}/\mathrm{d}z)\exp(6B/f_s^{(2)})\mathrm{d}z}{2B\sigma + f_s^{(2)2}\exp(2B/f_s^{(2)})}$$

$$> \frac{-4B}{\alpha D_s^{(2)}} \int_0^{\alpha} \frac{z(\mathrm{d}f_s^{(2)}/\mathrm{d}z)\exp 4B/f_s^{(2)})\mathrm{d}z}{f_s^{(2)2}}$$

$$= \frac{1}{D_s^{(2)}}\exp(4B/f_s^{(2)}(\alpha)) - 1$$

i.e. $D_s^{(2)} > \frac{1}{2}\exp[4B/f_s^{(2)}(\alpha)]$

which contradicts (68) and so $D_s^{(2)}$ cannot represent a stable solution.

TIME DEVELOPMENT

The solution to equation (48) is obtained for various values of B and α by a fourth order Runge–Kutta process on the function $\Gamma(z,t) = \delta^2(z,t)$. At $t = 0$, $\partial\Gamma/\partial t$ is undefined so we start with

$$\Gamma_0(\delta t) = 1 \tag{69}$$

$$\Gamma_1(\delta t) = 1 - \frac{3}{2}(B\delta t)^{1/2} \tag{70}$$

$$\Gamma_j(\delta t) = 1 - 2(B\delta t)^{1/2} \quad 2 \leqslant j \leqslant N, \quad N\delta z = \alpha \tag{71}$$

where $\Gamma_j(t) = \Gamma(j\delta z, t)$ is based on the solution of $\partial\Gamma/\partial t = 2B/\ln\Gamma$ for small t. The value of δt is chosen to ensure that the trajectory of $\delta(\alpha, t)$ (Fig. 2) starts near $\delta = 1$, giving δt as typically 0.01. The number of axial grid points, N, is 20. At each of the four substeps of the Runge–Kutta integration, $D(t)$ must be evaluated. The method chosen was an integration by Simpson's Rule. Then $(\partial T/\partial R)_{R=1}$ is evaluated using (50) or (53) for each grid point.

Figure 4 is an example of the growth of the solid crust where a steady-state is reached and Fig. 5 shows the development towards blockage in a pipe of the same length at a lower wall temperature. In Fig. 7 we show a curve giving critical values of B for a given α dividing blockage and non-blockage regimes.

The parameter α is typically very small and it would seem that the equation of the critical line is described to a good approximation by

$$B = 10^{-3/4}\alpha^{-7/20} \tag{72}$$

for $10^{-7} < \alpha < 10^{-3}$. Note that for a given fluid, physical changes and their effect on α and B can be briefly summarised by

Table 1. $\alpha = 10^{-5}$

B	$\delta_s(\alpha)$	D_s	t_s^*
0.20	0.9935	1.020	0.00297
1.20	0.9602	1.129	0.0225
2.20	0.9256	1.261	0.0450
3.20	0.8895	1.423	0.0675
4.20	0.8513	1.627	0.0975
5.20	0.8107	1.892	0.125
6.20	0.7669	2.250	0.160
7.20	0.7184	2.762	0.2025
8.20	0,6628	3.568	0.280
9.20	0.5936	5.085	0.410
10.20	0.4718	10.790	1.280
11.20	—	—	<0.25†
12.20	—	—	<0.15†
13.20	—	—	<0.10†

* Where t_s is the time taken to reach the steady-state ($|\partial\delta/\partial t| < 10^{-5}$).
† Denotes blockage times.

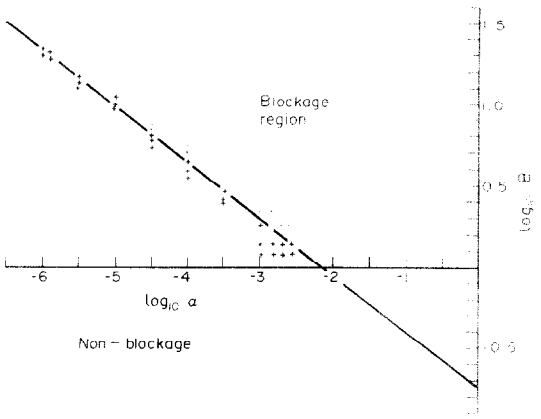

FIG. 7.

$$\frac{\Delta\alpha}{\alpha} = \frac{2\Delta l_0}{l_0} - \left(\frac{4\Delta r_0}{r_0} + \frac{\Delta P}{P}\right) \tag{73}$$

and

$$\frac{\Delta B}{B} = -\left(\frac{\Delta T_w}{T_m - T_w} + \frac{\Delta T_0}{T_0 - T_m}\right) \tag{74}$$

assuming constant fluid properties.

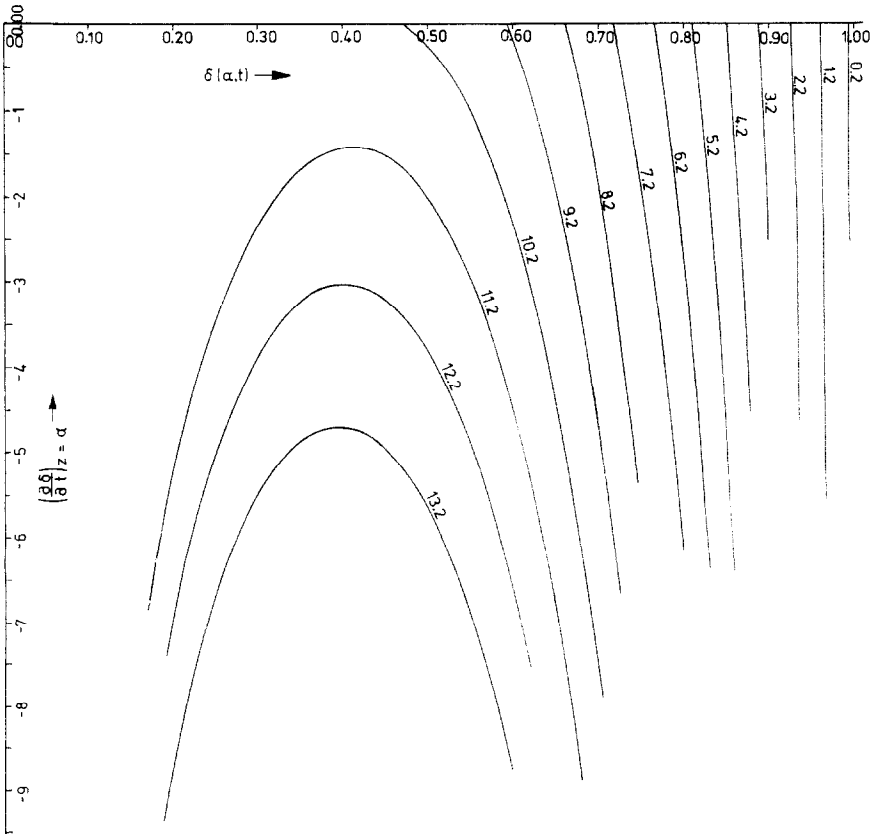

FIG. 6.

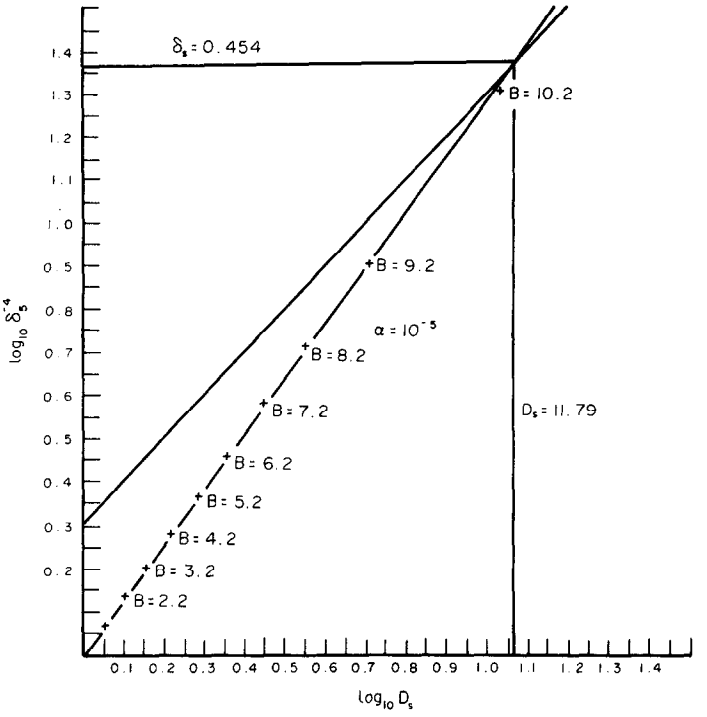

FIG. 8.

Table 1 presents results for a particular numerical experiment. The value of α was 10^{-5} and B was varied in the manner shown. The last three values of B led to the pipe blockage as the accompanying Fig. 6 (the phase-continuum diagram) shows. The time taken (in dimensionless 'seconds') for the system to reach steady-state is shown, along with the steady-state value D_s of $D(t)$ and the steady-state value $\delta_s(\alpha)$ of $\delta(\alpha, t)$ where applicable.

It was noted earlier that it is difficult to find the exact value of B for a given α which divides the blockage/non-blockage regions because the computation time increases as we approach this value. However, the previous stability analysis shows that the critical case corresponds to equation (57) having repeated roots. This permits us to define a dividing line in the α, B plane which separates blockage from non-blockage regions (see Fig. 7). We note that (66) can be rewritten as

$$D_s = \frac{1}{2}\Gamma_s^{-2}(\alpha) = \frac{1}{2}\delta_s^{-4}(\alpha). \tag{75}$$

To determine $\delta_s(\alpha)$ (the critical steady-state crust position at the nozzle exit) we draw a graph of (75) with $\log D_s$ as ordinate and $\log \delta_s^{-4}(\alpha)$ as abscissa for variable B. (This is a straight line through the point (0, log 2) with unit gradient.) If we then plot on the same graph some non-critical values of $\log D_s$ and $\log \delta_s^{-4}(\alpha)$ for fixed α, we obtain a further curve. The point of intersection of the two lines must then give the critical values of $\delta_s(\alpha)$ and D_s. Figure 8 shows results from Table 1 with critical values of 0.463 and 10.9 respectively.

COMPARISON WITH EXPERIMENT

Figure 9 shows some experimental results, taken from [6], where water at approximately 20°C has been passed through a pipe, at various values of wall temperature and inlet pressure. The solid symbols represent cases where blockage occurred and the open symbols denote steady-state solutions. Superimposed is a curve showing the dividing line between blockage and non-blockage derived from the theory presented in this paper. The value of the quantity $\rho\nu\kappa$ was taken, at the freezing point of water, to be 2.38×10^{-10} kg m s^{-2}. This is higher value than that which would have been used by Des Ruisseaux and Zerkle and so the values of α calculated for the experimental points are probably too high.

Some experiments on liquid steel are planned by British Steel at the Grangetown Laboratories. The experiments will be carried out with pipes of lengths between one and three feet and internal diameter of one inch. Vacuum suction will be used to supply the pressure drop. For liquid metals of Prandtl number 0.01 flowing through a pipe of aspect ratio $l_0/r_0 = 20$, the parameter $\alpha = 2000/Re_0$. With a thermal diffusivity of 2×10^{-5} m^2 s^{-1} and a density of 7500 kg m^{-3}, such a fluid, forced through a pipe of length 0.3 m by a pressure drop of 10^5 kg m^{-1} s^{-2}, will have a value of $\alpha \sim 2.1 \times 10^{-6}$. If this fluid has a melting point of 1700 K, enters the pipe at 1900 K where the wall temperature is 300 K, a value of B will be ~ 7 and it can be seen from Fig. 8 that a steady state solution will be

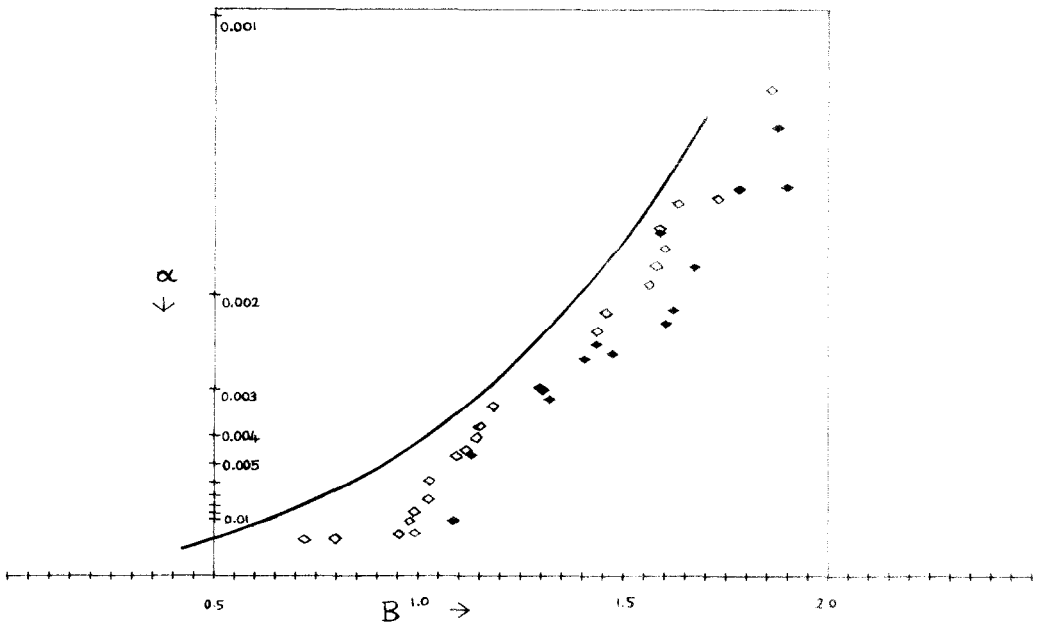

FIG. 9.

predicted. If the pipe length is quadrupled, we have blockage. However, as previously remarked, flow of liquid steel will be in most cases turbulent, highly desirable from the point of view of mixing and an even distribution of impurities. Because of these impurities, there will also be a 'mushy region' and not a single melting point. It is our intention to incorporate these modifications in new models.

REFERENCES

1. R. D. Zerkle and J. E. Sunderland, The effect of liquid solidification in a tube upon the laminar flow heat transfer and pressure drop, *J. Heat Transfer* **90C**, 183–190 (1968).
2. M. Epstein, A. Yim and F. B. Cheung, Freezing-controlled penetration of a saturated liquid into a cold tube, *J. Heat Transfer* **99C**, 233–238 (1977).
3. M. N. Özisik and J. C. Mulligan, Transient freezing of liquids in forced flow inside circular tubes, *J. Heat Transfer* **91C**, 385–389 (1969).
4. E. P. Martinez and R. T. Beaubouef, Transient freezing in laminar tube-flow, *Can. J. Chem. Engng* **50**, 445–449 (1972).
5. J. R. Sellars, M. Tribus and J. S. Klein, Heat transfer to laminar flow in a round tube or flat conduit the Graetz problem extended, *Trans. Am. Soc. Mech. Engrs* **78C**, 441–481 (1956).
6. N. Des Ruisseaux and R. D. Zerkle, Freezing of hydraulic systems, *Can. J. Chem. Engng* **47**, 233–237 (1969).
7. K. Stewartson and R. T. Waechter, On Stefan's problem for spheres, *Proc. R. Soc. A* **348**, 415–426 (1976).

UN MODELE MATHEMATIQUE DU BLOCAGE DE TUYERE PAR CONGELATION

Résumé—On présente un modèle mathématique qui décrit la formation d'une croûte sur la paroi interne d'un tube froid à l'intérieur duquel s'écoule un fluide. Une résolution numérique/analytique du problème de la solidification interne est donnée et on présente des critères qui donnent les conditions d'apparition d'un blocage.

EIN MATHEMATISCHES MODELL FÜR DIE BLOCKIERUNG EINER DÜSE DURCH GEFRIEREN

Zusammenfassung — Es wird ein mathematisches Modell vorgelegt, welches die Ausbildung einer Kruste an der Innenwand eines kalten Rohres beschreibt, das von einem Fluid durchströmt wird. Eine numerisch/analytische Behandlung des inneren Erstarrungsproblems wird durchgeführt und Kriterien angegeben, aus denen die Bedingungen ersichtlich sind, unter welchen Blockierung auftritt.

МАТЕМАТИЧЕСКАЯ МОДЕЛЬ БЛОКИРОВАНИЯ СОПЛА ПРИ ЗАСТЫВАНИИ ЖИДКОСТИ

Аннотация – Представлена математическая модель затвердевания жидкости на внутренней стенке охлаждаемой трубы. Дается численно-аналитическое решение задачи направленного внутрь процесса затвердевания и представлены критерии для определения условий возникновения блокировки сопла.